Direct and indirect roles of His-418 in metal binding and in the activity of β-galactosidase (*E. coli*)

Douglas H. Juers,[1] Beatrice Rob,[2] Megan L. Dugdale,[2] Nastaron Rahimzadeh,[2] Clarence Giang,[2] Michelle Lee,[2] Brian W. Matthews,[1] and Reuben E. Huber[2]*

[1]Instititute of Molecular Biology, Howard Hughes Medical Institute and Department of Physics, University of Oregon, Eugene, Oregon 97403-1229

[2]Division of Biochemistry, Faculty of Science, University of Calgary, Calgary Alberta, Canada, T2N 1N4

Received 2 January 2009; Revised 2 April 2009; Accepted 9 April 2009
DOI: 10.1002/pro.140
Published online 16 April 2009 proteinscience.org

Abstract: The active site of ß-galactosidase (*E. coli*) contains a Mg^{2+} ion ligated by Glu-416, His-418 and Glu-461 plus three water molecules. A Na^{+} ion binds nearby. To better understand the role of the active site Mg^{2+} and its ligands, His-418 was substituted with Asn, Glu and Phe. The Asn-418 and Glu-418 variants could be crystallized and the structures were shown to be very similar to native enzyme. The Glu-418 variant showed increased mobility of some residues in the active site, which explains why the substitutions at the Mg^{2+} site also reduce Na^{+} binding affinity. The Phe variant had reduced stability, bound Mg^{2+} weakly and could not be crystallized. All three variants have low catalytic activity due to large decreases in the degalactosylation rate. Large decreases in substrate binding affinity were also observed but transition state analogs bound as well or better than to native. The results indicate that His-418, together with the Mg^{2+}, modulate the central role of Glu-461 in binding and as a general acid/base catalyst in the overall catalytic mechanism. Glucose binding as an acceptor was also dramatically decreased, indicating that His-418 is very important for the formation of allolactose (the natural inducer of the *lac* operon).

Keywords: β-galactosidase; magnesium; degalactosylation; galactosylation; sodium

Introduction

β-Galactosidase (EC 3.2.1.23) from *E. coli* is a tetrameric enzyme that catalyzes hydrolytic and transgalactosidic reactions[1] on β-D-galactopyranosides.[2] Substrates initially bind in a "shallow" mode,[3,4] subsequently moving deeper into the active site so that the glycosidic oxygen is close enough to be protonated by Glu-461 (general acid catalysis) and the galactosyl anomeric carbon is close enough to contact the nucleophile, Glu-537. A carbocation-like transition state forms that collapses into an α-galactosidic bond between the carboxyl of Glu-537 and the C1 of galactose. This first step of the reaction, with rate constant k_2 (see Fig. 1), is called galactosylation (the enzyme becomes galactosylated).

Upon glycosidic bond cleavage, the first product normally diffuses away. Water or an acceptor with a

Abbreviations: Amp, ampicillin; BSA, bovine serum albumin; DMSO, dimethyl sulfoxide; EDTA, ethylene diamine tetraacetic acid; Glc, glucose; IPTG, isopropyl-thio-ß-D-galactopyranoside; oNP, o-nitrophenol; oNPG, o-nitrophenyl-ß-D-galactopyranoside; PETG, phenylethyl-thio-ß-D-galactopyranoside; pNP, p-nitrophenol; pNPG, p-nitrophenyl-ß-D-galactopyranoside; TES, N-tris(hydroxymethyl) methyl-2-aminoethane-sulfonic acid; T-oNPG, thio-o-nitrophenyl-ß-D-galactopyranoside.

Douglas H. Juers's current address is Department of Physics, Whitman College, Walla Walla WA 99362, USA.

Grant sponsor: NIH; Grant number: GM20066; Grant sponsor: National Science and Engineering Research Council (Canada); Grant number: 4691.

Correspondence to: Reuben E. Huber, Division of Biochemistry, Faculty of Science, University of Calgary, Calgary Alberta, Canada T2N 1N4. E-mail: huber@ucalgary.ca

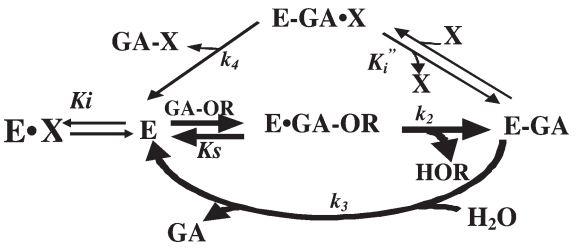

Figure 1. Postulated reaction mechanism of β-galactosidase. The thick arrows represent the reaction without inhibitor (or acceptor). The thin arrows represent the additional reactions that occur when inhibitor/acceptor is present. E = β-galactosidase; X = inhibitor/acceptor; GA-OR = β-galactoside substrate; GA = galactose; GA-X = galactosyl-inhibitor/acceptor adduct; k_2 = galactosylation rate constant; k_3 = degalactosylation rate constant; *Ks* = dissociation constant for E•GA-OR; K_i = competitive inhibition constant representing the dissociation of E•X; K_i'' = dissociation constant for E-GA•X; k_4 = transgalactosylation rate constant. The dots indicate that some sort of complex exists with the enzyme. The hyphens indicate a covalent bond.

hydroxyl group then enters and is activated by Glu-461 via general base catalysis. The galactosyl moiety is released to this molecule via a second carbocation-like transition state (the two transition states are thought to be similar) to form free galactose or an adduct having a galactosidic bond with the acceptor. The rate constant for this step is k_3 if the reaction is with water (called degalactosylation) or k_4 if the reaction is with an acceptor (called transgalactosylation). When lactose is the substrate, some of the Glc (first product) remains bound long enough to react as the acceptor,[1] in which case the product is allolactose, the natural inducer of the lac operon.

β-Galactosidase requires Mg^{2+} or Mn^{2+} for full catalytic activity,[5–7] but the exact role of this ion in catalysis is unclear.[3,8–10] The active site also includes a monovalent cation (usually either Na^+ or K^+) important for activity, which directly ligates the galactosyl O_6 hydroxyl during catalysis.[3,11] The two ion sites are situated a few Å apart in the active site, both very near to an interface between two domains of the protein.

Crystal structure and site directed mutagenesis experiments have shown that His-418, along with Glu-416 and Glu-461 (the acid/base catalyst) are ligands to the Mg^{2+} at the active site.[12–15] Besides ligating the Mg^{2+} ion, His-418 is one of several residues that together form an opening that guides substrates into the binding site (see Fig. 2 16), and it is thought to contact the aglycone moeity of the substrate, pointing to a possible role in the formation of allolactose.[3] His-418 is also close to Glu-461, and so very likely directly impacts the properties of that important catalytic residue.

To better understand the role of His-418 and of Mg^{2+}, we substituted His-418 with Asn, Glu and Phe and characterized the variants structurally and biochemically. A Glu at site 418 probes the effect of having three carboxyl ligands to the active site Mg^{2+}. The Asn side chain at site 418 was expected to be an architectural mimic of His with respect to binding Mg^{2+} - both side chains are neutral and the oxygen of the Asn amido group[17] could substitute for the ND1 of His-418. Phe was substituted because it roughly retains the size, shape and aromatic[18] characteristics of His, but would not be expected to ligate to Mg^{2+}.

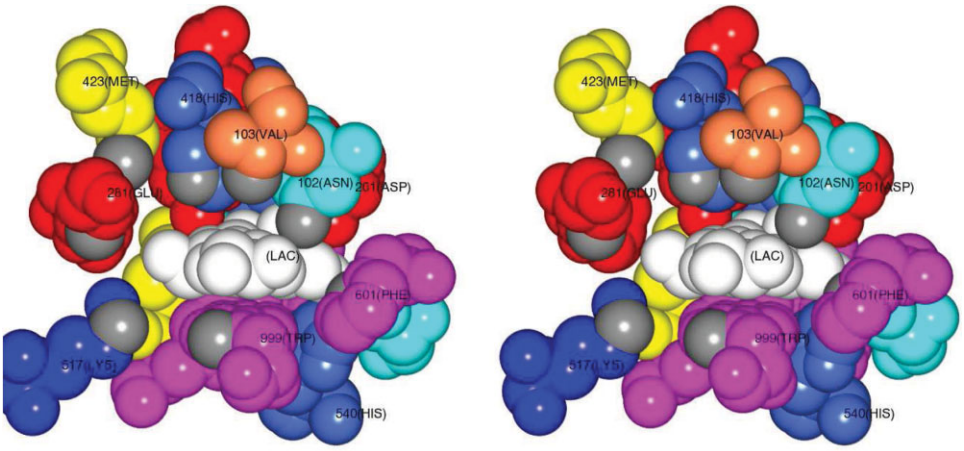

Figure 2. Stereo representation of the active site pocket of β-galactosidase with a bound lactose molecule (white). The coordinates used for the figure are from Protein Data Bank file 1JYN for the complex between the inactive E537Q variant and lactose. All residues that contribute atoms to the pocket are shown color coded by residue property (magenta = aromatic, coral = nonpolar, yellow = methionine, blue = basic, cyan = polar, red = acidic). Grey atoms are those used to define the opening to the pocket (see text). Residues 418, 103, 102, and 201, which all pack together to form part of the "top" surface of the pocket, are disrupted by the substitution of His-418 with glutamate (see text). The active site ions are not visible in the figure but lie behind the sidechains of His-418 (Mg^{2+}) and Asp-201 (Na^+) (Figure prepared with CCP_4 mg.[16])

Table I. *Crystallographic Data Collection and Refinement Statistics for His-418 Substituted β-Galactosidases*

Variant	Resolution (Å)	<I>/<σ>	Completeness (%)	Redundancy	R_{sym} (%)	R_{meas} (%)
H418N	28.7–1.75	10.8 (4.2)	96.8 (84.5)	2.7	4.4 (17.3)	5.4 (21.3)
H418N/IPTG	30.0–1.80	6.9 (2.0)	98.0 (94.6)	3.2	8.9 (42.2)	7.6 (36.2)
H418E	34.5–2.05	7.9 (2.4)	99.4 (98.2)	2.6	8.0 (31.6)	10.0 (40.1)
H418E/Gal	500–3.0	5.1 (1.6)	91.7 (94.2)	1.8	12.3 (47.8)	74 (67)

				Deviations from ideal values		
	Cell parameters (Å)	Wilson B-factor (Å²)	R-Factor (%)	Bond lengths (Å)	Bond angles (degrees)	Avg B (MC protein, Å²)
H418N	149.4 168.0 200.3	15.4	15.9	0.017	2.85	19.3
H418N/IPTG	152.0 162.5 204.0	18.9	17.3	0.016	2.83	21.6
H418E	149.3 167.2 200.4	20.1	15.8	0.015	2.88	23.8
H418E/Gal[a]	128.4 152.9 132.1	60.0	21.8	0.007	1.37	42.3
Native[b]						16.8
Native/IPTG						22.4

Data for (H418N, H418N/IPTG and H418E) were collected at the Stanford Synchrotron Radiation Laboratory Beamline 7-1. Data for H418E/Gal were collected at the Advanced Light Source in Berkeley (California) at beamline 8.3.1 under agreement with the Alberta Synchrotron Institute* and processed using Mosflm and Scala. <I>/<σ> gives the average intensity relative to the average uncertainty, with the high resolution bin in parentheses. R_{sym} gives the agreement between equivalent reflections. R_{meas} is a multiplicity weighted agreement between equivalent reflections. Avg B gives the average mainchain protein B-factor after refinement.

[a] H418E/Gal was solved in a monoclinic space group ($P2_1$) with $\beta = 102.7^\circ$. This was crystallized under the same conditions as the other variants, and was refined using CNS with a different geometry library and weighting scheme from the other structures.

[b] The structures of native enzyme (1DP0) and native enzyme with IPTG bound (1JYX) were determined previously. The B-factors are given here for comparison.

Results

Crystal structures

Structures were determined of the following variants: H418N with and without bound IPTG, and H418E with and without bound galactose (Table I). Overall, the structures of H418N- and H418E-β-galactosidase are very similar to that of the native enzyme (see Fig. 3). Rms deviations in main chain positions are in the range of 0.05–0.2 Å at the tetramer, monomer and domain levels. For both mutants the Mg^{2+} remains bound with octahedral ligation as in the native protein.[20] With H418N-β-galactosidase, the Asn side chain is nearly "isoteric" with His. The crystallographic analysis does not differentiate between the nitrogen and oxygen of the side chain although Mg^{2+} usually prefers oxygen over nitrogen as a ligand. With H418E-β-galactosidase, the extra methylene group in the Glu side chain results in a slight distortion of the Mg^{2+} site. For both variants, the Na^+ site has distorted square pyramidal geometry as in native, including three protein ligands and two waters or one water and the 6-OH from the sugar.

There are differences in the B-factors between the structures. In particular, the main-chain B-factors of H418E increase on average by 45% relative to native and those residues with the greatest increase are concentrated near the active site on several loops (see Fig. 4). Furthermore, of the 1011 residues in the structure, five of the seven highest side chain B-factor increases occur at positions 418, 103, 461, 201, and 102, all localized near the Mg^{2+} and Na^+ binding sites (Figs. 2 and 3). This localization is not as evident with H418N. Although this variant shows an average 16% main chain B-factor increase relative to native enzyme, the residues with the highest B-factor increases are more evenly dispersed throughout the molecule (see Fig. 4).

A more subtle change is a small increase in the size of the opening of the active site. In the case of H418E this was suggested by a relative shift of 0.2 Å or so by atoms on opposite sides of the opening to the active site pocket. The H418N variant has a much smaller overall expansion but the size of the opening increases because the smaller side-chain at site 418 (Asn vs. His) removes two atoms from the opening surface (Figs. 2 and 3).

The structure of the complex between H418N and IPTG was determined (not shown). This showed IPTG to bind essentially identically as it does to native, although with slightly higher B-factors.

In a further crystallographic study (resulting in a different space group), D-galactose was shown to bind to H418E in a position similar to native enzyme. There was, however, a second galactose bound in the active

*The Advanced Light Source at Lawrence Berkeley lab is operated by the Department of Energy (U.S.A.) and supported by the National Institute of Health (U.S.A.). The National Science Foundation, the University of California and Henry Wheeler fund Beamline 8.3.1. The Advanced Light Source synchrotron access program is supported by grants from the Alberta Science and Research Authority and the Alberta Heritage Foundation for Medical Research.

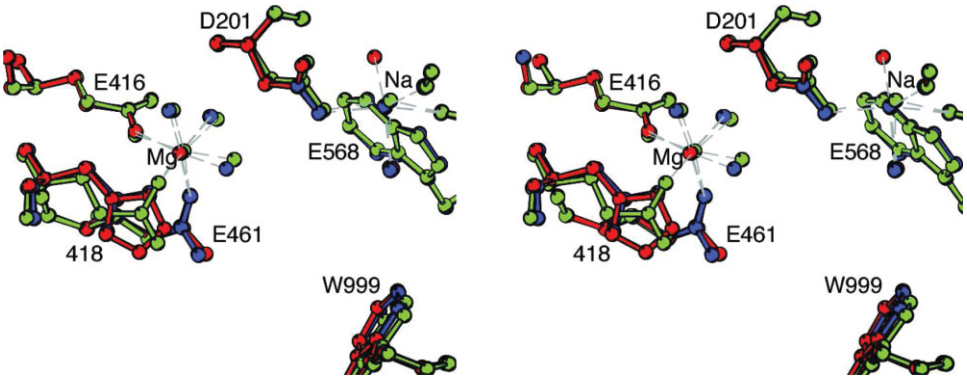

Figure 3. Stereoview showing the active site Mg^{2+} and Na^{+} binding sites. Both are changed only very subtly by substituting for His-418 in the native structure (red) with either Asn (blue) or Glu (green). The substrate will bind initially in the lower left between positions 418 and 999. (Figure prepared with Molscript.[19])

site of H418E (where an acceptor might bind) at a site (see Fig. 5) not occupied in the complex with the native enzyme. Glu-418 makes a hydrogen bond to the second galactose, apparently contributing directly to its binding.

Overall effects on activity

Because some of the effects on activity are complicated and interdependent it may help to give an overall summary first, and then to present the results in more detail.

1. The substituted enzymes have 4–100× lower k_{cat} and up to about 1000× higher K_m than native enzyme, and in most cases no longer distinguish between ONPG and PNPG (Table II).
2. Na^{+} binds 8× and 5000× more poorly to H418N and H418E, respectively, than to native.
3. Mg^{2+} binds a few fold better and a few fold worse to H418N and H418E, respectively. (The latter is reversed with high Na^{+} concentrations.)

Effects of Na^{+} and Mg^{2+} on kinetic constants

To determine the affinity of the ions for their binding sites, k_{cat} and K_m were determined as a function of the ion concentrations and fit to simple two-state binding curves (Figs. 6 and 7). These results are summarized in Table III.

For most cases, k_{cat} was insensitive to either Mg^{2+} or Na^{+}, the exception being H418E vs Na^{+}. K_m usually decreased with increasing ion concentration, but increased for H418E and H418F with Mg^{2+}. H418E-β-

*The Advanced Light Source at Lawrence Berkeley lab is operated by the Department of Energy (U.S.A.) and supported by the National Institute of Health (U.S.A.). The National Science Foundation, the University of California and Henry Wheeler fund Beamline 8.3.1. The Advanced Light Source synchrotron access program is supported by grants from the Alberta Science and Research Authority and the Alberta Heritage Foundation for Medical Research.

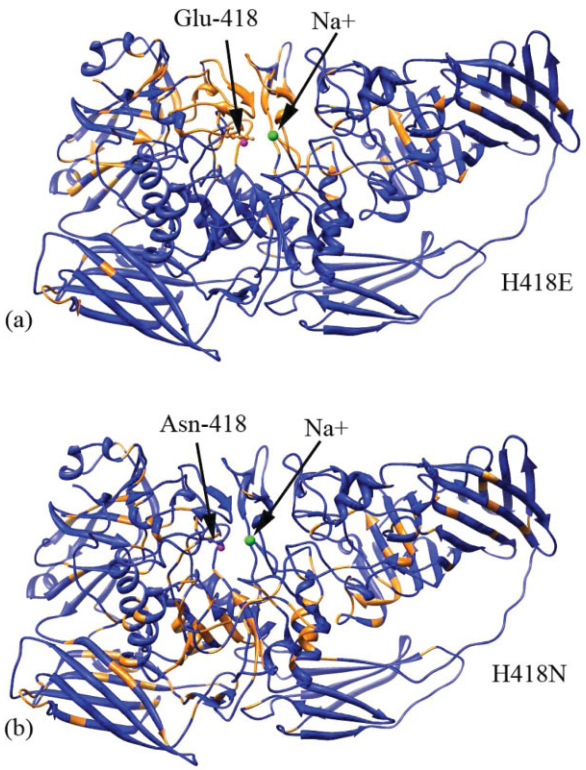

Figure 4. Color-coded ribbon representations of the β-galactosidase subunit showing the increase in B-factors with the H418 substitutions compared to native enzyme. For each residue, the B-factors were averaged over the mainchain atoms and the four subunits in the tetramer. Orange represents the ~160 residues with the greatest increase, with the rest in blue. The two active site metal ions are shown as spheres with Na^{+} in green and Mg^{2+} in magenta. The latter is located just behind the sidechain at position 418, shown in balls and sticks. (a) The H418E variant, for which the orange residues correspond to >62% B-factor increase over native enzyme. These are mostly localized nearby the active site. (b) The H418N variant, for which orange residues residues correspond to >22% B-factor increase. These are distributed more uniformly throughout the molecule. (Figure prepared with UCSF Chimera.[22])

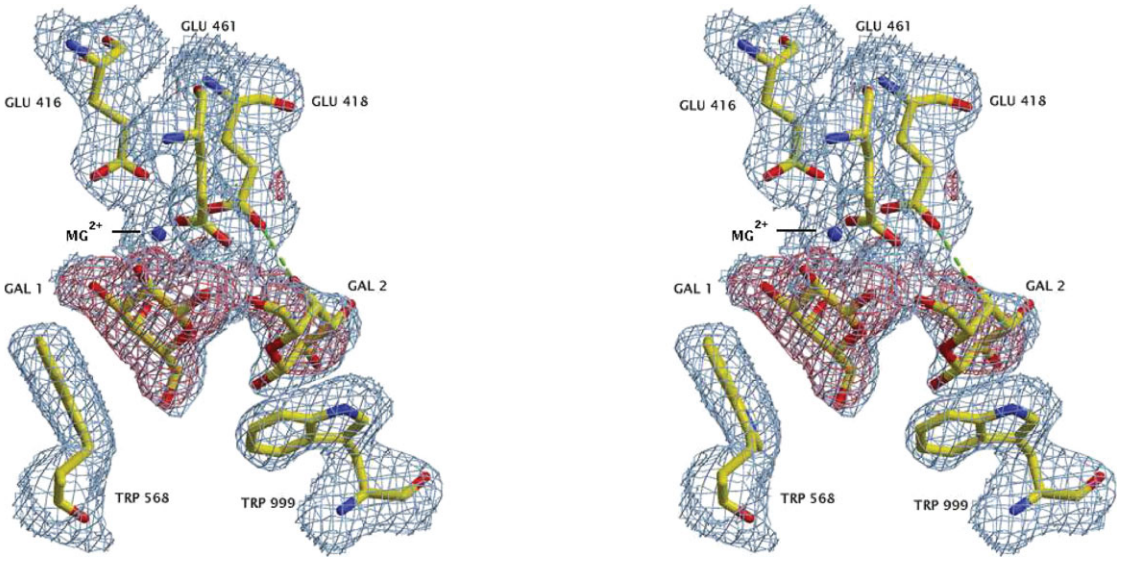

Figure 5. Stereoview showing the electron density ($2f_o$-f_c, contoured at 1s—shown as blue netting) and the positions of the two galactoses that bind to the active site of the H418E variant. The red netting is positive (3s) f_o-f_c "omit" electron density. Here, f_o refers to amplitudes measured from the galactose-soaked crystals, while f_c (and the phases) are calculated from a model of the H418E variant with no waters or sugars in the active site and refined against the f_os. A putative hydrogen bond between Glu-418 and the O_4 of the galactose binding in the acceptor position is shown as a dashed green line. Gal 1 refers to the galactose bound as it does to the native while Gal 2 is the galactose that binds to this variant but not to native. The stick model based on the refined coordinates is also shown. Oxygens are in red, carbons are in yellow and nitrogens are in blue. The active site Mg^{2+} is shown as a blue ball. [Figure was prepared with ImageMagick (*www.imagemagick.org*).] [Color figure can be viewed in the online issue, which is available at www.interscience.wiley.com.]

Galactosidase bound Na^+ very poorly, hence measurements to characterize this variant were done both at 150 m*M* and 2*M* NaCl. Activity increased at 2*M* NaCl, and from the curve in Figure 6(B), the k_{cat} at saturating NaCl would be about 35 s^{-1}. The k_{cat} at 2*M* NaCl is about 25 s^{-1}, which is not too much lower.

Competitive inhibition

Compared to native enzyme, H418E-β-galactosidase at both 150 m*M* and 2*M* Na^+ was inhibited very poorly by lactose and the substrate analogs (PETG, IPTG, T-oNPG) while transition state analogs (D-galactonolactone†, L-ribose) inhibited about the same (or better) (Table IV). D-Galactose and L-arabinose inhibited this enzyme better than native. The inhibition of H418N-β-galactosidase mirrored the inhibition by H418E-β-galactosidase except that the loss of inhibition by the substrate analogs was smaller. H418F-β-Galactosidase was inhibited very poorly by all of the inhibitors tested.

The temperature dependencies of the binding constants (K_{bind}) of IPTG, PETG, and D-galactose to native and H418N-β-galactosidase were obtained (see Fig. 8). Since K_i is an inhibitor dissociation constant, $1/K_i$ is the corresponding binding constant ($1/K_i = K_{bind}$). The slopes of $\ln(1/K_i)$ vs $\ln(1/T)$, which are indicative of ΔH_o (binding), were all smaller with H418N-β-galactosidase than with native enzyme. Thus, the enthalpy of binding decreases as a result of the substitution. Table V summarizes the thermodynamic analysis. The more positive (less favorable) ΔH_o values for binding to H418N-β-galactosidase compared to native were incompletely compensated by more positive (more favorable) ΔS_o (and $T\Delta S_o$) values and thus binding was worse. The effects on D-galactose were similar but the enthalpy was not decreased as much as for IPTG and PETG, which accounts for its better binding to H418N-β-galactosidase.

Effects of acceptors on the rates

First order increases in k_{cat}, with respect to the concentration of 1-propanol (data not shown), a very reactive acceptor of native β-galactosidase,[23] were observed, suggesting that the rate at high [acceptor] is very large. Similar effects were observed with Glc for each substituted enzyme except for H418E-β-galactosidase at 2*M* NaCl (data also not shown). In that case, $appk_{cat}$ was hyperbolic and the [Glc] at which the rate increased to half the final value [Eq. (4)] was 335 m*M*.

†D-Galactonolactone has a high Ki (~0.6 m*M*) for a transition state analog. However, δ-1,5-galactonolactone, the only D-galactonolactone form that binds at the active site NMR,[21] is present in such small amounts in solutions of D-galactonlactone that it is not detectable by NMR (3). The γ-1,4-galactonolactone form predominates. Thus, δ-1,5-galactonolactone binds with the very high affinity expected of a transition state analog. The *Ki* of L-ribose (~0.2 m*M*) is also high. However, this is a pentopyranose without a C6 hydroxyl. Such sugars usually have *Ki* values well over 100 m*M*.[2] The K_i value of L-ribose is small relative to such values. It is also known that L-ribose binds to the enzyme in a similar way that a transition state would be expected to bind (unpublished observation).

Table II. *Kinetic Constants of Native and Mutant β-Galactosidases with oNPG and pNPG*

	Native	H418E 0.01 m*M* Mg^{2+} 150 m*M* Na^+	H418E 0.01 m*M* Mg^{2+} 2*M* Na^+	H418N 0.01 m*M* Mg^{2+} 150 m*M* Na^+	H418F 10 m*M* Mg^{2+} 150 m*M* Na^+	Mg^{2+} free[a]
pNPG						
k_{cat} (1/s)	90.0 ± 1.0	5.4 ± 0.7	22.0 ± 1.0	5.5 ± 0.2	10.3 ± 0.4	17
K_m (mM)	0.04 ± 0.004	13.2 ± 1.3	0.21 ± 0.04	0.05 ± 0.01	20.8 ±1.2	0.12
oNPG						
k_{cat} (1/s)	620 ± 7	5.4 ± 0.7	24.6 ± 0.6	4.9 ± 0.2	10.4 ± 0.8	80
K_m (mM)	0.12 ± 0.01	104 ± 21	0.22 ± 0.02	0.06 ± 0.01	30.6 ± 2.3	0.62

Except for H418F-β-galactosidase, which was studied at relatively high Mg^{2+}, the studies were done at 0.01 m*M* Mg^{2+} which avoids the effects of the second catalytically important Mg^{2+} binding site on the k_{cat}.[7]
[a] Ref. 3.

This means that $((k_2 + k_3)/(k_2 + k_4))K_i''$ is 335 m*M*. Since k_3 is smaller than k_4 (shown by the increase in rate with [Glc]), K_i'' (see Fig. 1) is >335 m*M*. Glc thus binds very poorly in every case.

pH profiles

The substitutions caused significant changes to the pH rate profiles (see Fig. 9). H418E-β-Galactosidase was only poorly reactive at pH 7.0 with low (150 m*M*) [Na^+] but, unexpectedly, its k_{cat} increased as the pH increased with a mid-point at about pH 9.2. At 2*M* NaCl, the k_{cat} decreased as the pH increased with a mid-point of about 7.7. H418N-β-Galactosidase had relatively low activity at pH >7.0, but the k_{cat} value increased as the pH was lowered below 7 (the enzyme cannot be easily assayed at pH below 6 because of the low extinction coefficient of oNP at those pH values and because the enzyme starts becoming unstable—thus the exact amount that the pKa is lowered is uncertain). The pH profile of H418F-β-galactosidase is very similar to that of native β-galactosidase in the absence of Mg^{2+}.[24]

Discussion

Role of His-418 in binding Mg^{2+} and Na^+

In native β-galactosidase, His-418 is a ligand to the principal active site Mg^{2+} ion. The other two protein residues are Glu-416 and Glu-461. H418N-β-Galactosidase bound Mg^{2+} a little better than native enzyme, which is not unexpected, since His-418 and Asn-418 are "isoteric" for the configuration used in ligating the Mg^{2+} ion (see Fig. 3). H418E-β-Galactosidase bound Mg^{2+} approximately 10-fold worse at 150 m*M* NaCl but binding was similar to native at 2*M* NaCl. Oxygen is preferred over nitrogen as a Mg^{2+} ligand,[17] but the longer side-chain of the glutamic acid results in poorer ligating geometry.

Although the direct effect of the H418E mutation is at the Mg^{2+} site, it also weakens Na^+ binding almost 5000-fold. Increasing NaCl from 0.15 to 2*M* restored Mg^{2+} binding about 10-fold—to its level with native enzyme (Fig. 7 and Table III). The poor Na^+ binding can be attributed to the poorer ordering of a subset of the residues that line the active site opening: Glu-418, Val-103, Asn-102, and Asp-201 (Figs. 2 and 4). The side chains of these four residues pack together to connect the two cation binding sites, and they undergo the largest B-factor increases in the structure as a result of the substitution, indicating that the disruption of the Mg^{2+} binding site is propagated to the Na^+ binding site through this group of residues. These residues may also be easy to disrupt because they lie at a domain interface. In the case of H418N, the effect on Na^+ binding is much smaller (8× vs. 5000×), and there is less crystallographic evidence for this disruption. With native enzyme, there is some

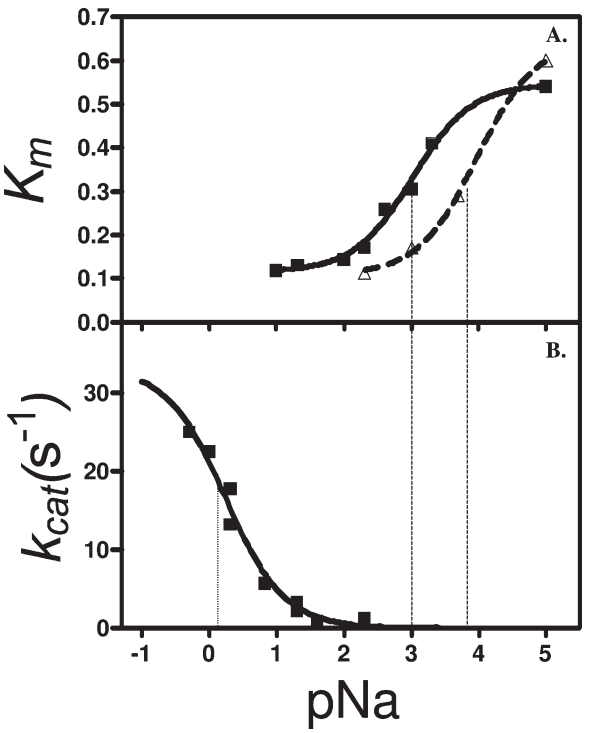

Figure 6. A. The changes of the K_m values (m*M*) of H418N- and native β-galactosidase as functions of pNa. The triangles (dashed line) represent native β-galactosidase and the squares (solid line) represent H418N-β-galactosidase. B. The k_{cat} values (s^{-1}) of H418E-β-galactosidase as a function of pNa. The thin perpendicular lines on the plots show the pNa_{mid} values.

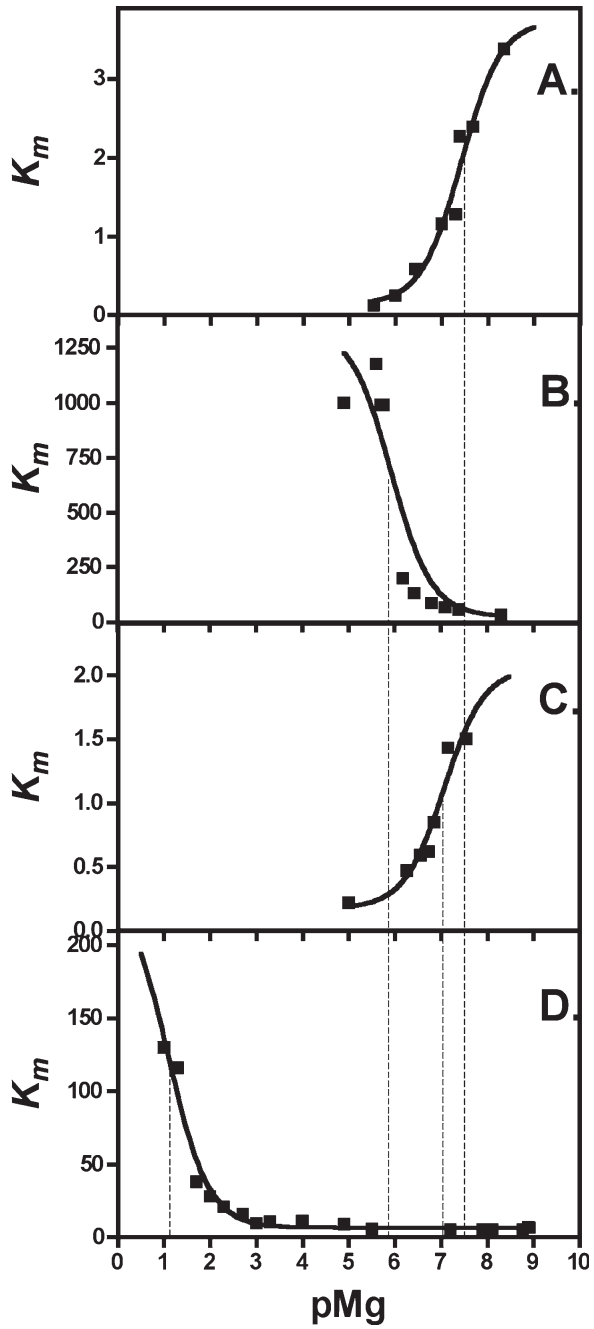

Figure 7. Plots of the K_m values (m*M*) as functions of pMg. (A) H418N-β-galactosidase. (B) H418E-β-galactosidase at 150 m*M* NaCl. (C) H418E-β-galactosidase at 2*M* NaCl. (D) H418F-β-galactosidase. Thin dashed lines indicate the pMg_{mid} values.

previous evidence that the affinity of the protein for one ion is affected by the presence of the other.[25,26]

Loss of the ability to bind Na^+ can alter the binding of substrates and the stabilization of the transition state and thus the activity of the enzyme.[3,11,20] This ion is probably also important for movement of the substrate from the shallow mode to the deep mode.[3] However, in contrast to the improved binding of Mg^{2+}, the binding of substrate and transition state analogs to H418E was not affected significantly when the [Na^+] was increased to 2*M* (Table III).

Role of His418 in substrate binding

The affinity of the active site of the His-418 substituted enzymes for substrate analogs decreased by 40–5000× (equivalent to 9–20 kJ/mol less binding energy). Based on the structure of the complex between H418N and IPTG, these substitutions have very small effects on the position and configuration of the bound substrate analogs. All of the specific interactions with the protein are the same as with native enzyme. Furthermore, while it has been proposed that a role of Mg^{2+} is to orient active site residues for correct binding and catalysis,[9,27–29] the Glu and Asn substitutions have very small effects on the position and configuration of the Mg^{2+} ion. Thus, orientation changes are not the reason for the poor substrate binding and activity.

There are two galactosyl hydroxyls on the substrate most likely to be affected by substitutions at position 418. First, the O_4 hydroxyl interacts with a water molecule ligated to the Mg^{2+}. Substitutions at position 418 could alter the electronic properties of the water via the Mg^{2+}. Second and probably more important, the O_2 hydroxyl makes a hydrogen bond to Glu-461, which also is ligated to the Mg^{2+}. It is likely that the binding properties of Glu-461 are altered by substitution for His-418; either via the Mg^{2+} or through direct interaction between residues 418 and 461, since they are close to each other. The enthalpy (ΔH_o) released (Fig. 8 and Table V) upon binding substrate analog inhibitors (IPTG and PETG) was decreased by 24 kJ/mol as a result of substituting Asn for His-418, indicating that the bonds with the water molecule and/or with Glu-461 are weaker. Averaged over the four subunits, the B-factors of the O_2 hydroxyl increased by ~40% over the native/IPTG complex, while the other three hydroxyls increased no more than ~20%, consistent with weakened contacts between this group and Glu-461.

While the enthalpy of binding becomes less favorable - probably through weakened interactions with Glu-461—the entropy of binding was more favorable for

Table III. *Dependence of k_{cat} and K_m on Ion Concentrations*

	k_{cat} dependence		K_m dependence	
Variant	On Mg^{2+} (μ*M*)	On Na^+ (m*M*)	On Mg^{2+} (μ*M*)	On Na+ (m*M*)
Native	+0.1[a]	+0.36[b]	−0.1[a]	−0.12[b]
H418N	none	none	−0.03	−0.98
H418E	none	+575	+1.3 (-0.1)[c]	−575
H418F	none	(no data)	+10⁴	(no data)

The sign (+ or −) indicates a direct or inverse dependence, and the number gives the metal binding constant.
[a] Ref. 7.
[b] Ref. 11.
[c] With 2*M* NaCl.

Table IV. *Competitive Inhibition Constants (K_i (mM)) of Native and Substituted β-Galactosidases*

	Native 0.01 m*M* Mg	H418E 0.01 m*M* Mg^{2+}	H418E 0.01 m*M* Mg^{2+} 2*M* Na^{+}	H418N 0.01 m*M* Mg^{2+}	H418F 10 m*M* Mg^{2+}
lactose	0.9	13	55	5.1	880
PETG	0.002	10	5	0.08	10
IPTG	0.08	85	45	5.0	223
t-ONPG	0.025	8.4	—	4.2	—
D-galactonolactone	0.64	0.40	0.64	0.40	—
2-amino-galactose	1.0	1.3	0.7	1.4	—
L-ribose	0.28	1.4	1.5	0.68	140
D-galactose	21	3.4	4.8	3.3	94
L-arabinose	220	130	120	25	—

Unless otherwise indicated, the studies were done at 150 m*M* NaCl. The standard errors were less than 15% in every case. Note that even though lactose is a substrate of ß-galactosidase, it reacts very slowly compared to oNPG or pNPG and its ability to act as a competitive inhibitor can be measured.

the substituted enzyme by 14 kJ/mol ($T\Delta S_o$ at 25°C—Table V). This can be explained by the extra space created in the active site pocket upon substitution. The residues lining the active site opening include the residues that constrain the position of the aglycon after binding. With a somewhat less snug fit, the aglycon will have greater mobility in the bound state, reducing the entropic cost of binding. This mobility may in turn help to weaken enthalpic contributions to binding by partially disrupting hydrogen bonds between the enzyme and galactosyl hydroxyls. There could also be greater displacement of solvent molecules in the bound state, which will increase the entropy of binding. These effects are likely to be more significant with the H418E variant. In this case, the residues lining the active site opening are more mobile, including Asn-102, which makes a hydrogen bond to the galactosyl ring oxygen in the IPTG complexes. This helps to explain why this variant binds substrate analogs 10–100× worse than the H418N variant. Furthermore, since transition state analogs bind deeper in the active site and away from the mobile residues at the pocket opening, they would be unable to take advantage of this entropic effect and would not be affected by a poorer interaction with Asn-102, helping to explain why their affinity is essentially unaffected by the substitutions.

Galactose binds to H418E in a manner similar to native (see Fig. 5). However, with H418E, a second galactose molecule is bound in the active site. Its O_4 hydroxyl interacts with the carboxylate side chain of Glu-418, and the O_6 hydroxyl is close to the C1 of the first galactose—in a manner that would be expected if this galactose were the acceptor. The interactions of the second galactose do not occur with native enzyme. The N3 of His-418 must either not be in the proper position or does not have the correct electronic properties to bind the second galactose. The binding of a second galactose helps to explain the anomalously high affinity of galactose for the Glu-418 variant.

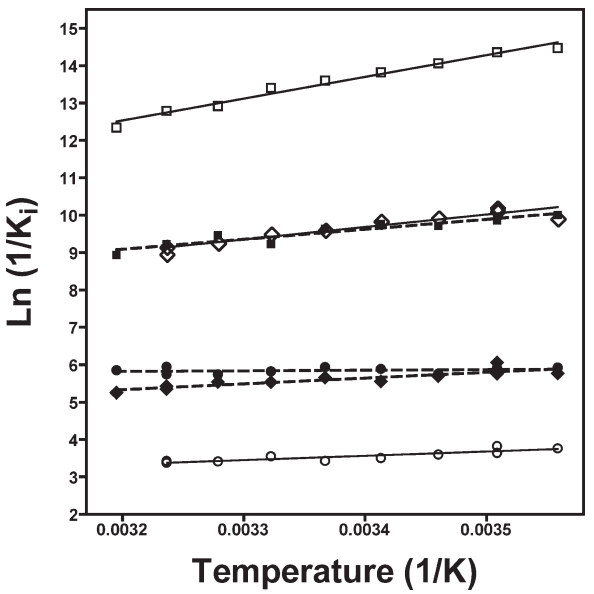

Figure 8. van't Hoff plots of the binding of IPTG, PETG and D-galactose to native and H418N-β-galactosidase. The units of the K_i values are *M* and ln(1/K_i) is plotted versus 1/absolute temperature (K). Open squares and solid line, PETG with native; solid squares and dashed line, PETG with H418N-β-galactosidase; open diamonds and solid line, IPTG with native; solid diamonds and dashed line, IPTG with H418N-β-galactosidase; open circles and solid line, D-galactose with native; solid circles and dashed line, D-galactose with H418N-β-galactosidase.

Table V. *Thermodynamic Data for Binding of Inhibitors to Native, and H418N-β-Galactosidases*

	Native		H418N-β-galactosidase	
	ΔH_o (kJ/mol)	$T\Delta S_o$ (kJ/mol)	ΔH_o (kJ/mol)	$T\Delta S_o$ (kJ/mol)
IPTG	−33.8	−10.2	−10.1 (+23.7)	3.6 (+13.8)
PETG	−44.7	−11.0	−21.0 (+23.7)	2.6 (+13.6)
D-galactose	−10.0	−1.3	−1.3 (+8.7)	13.2 (+14.6)

These were obtained by the use of the van't Hoff plot (Figure 8). Changes in the values of the activation thermodynamics for H418N-ß-galactosidase relative to native are shown in brackets.

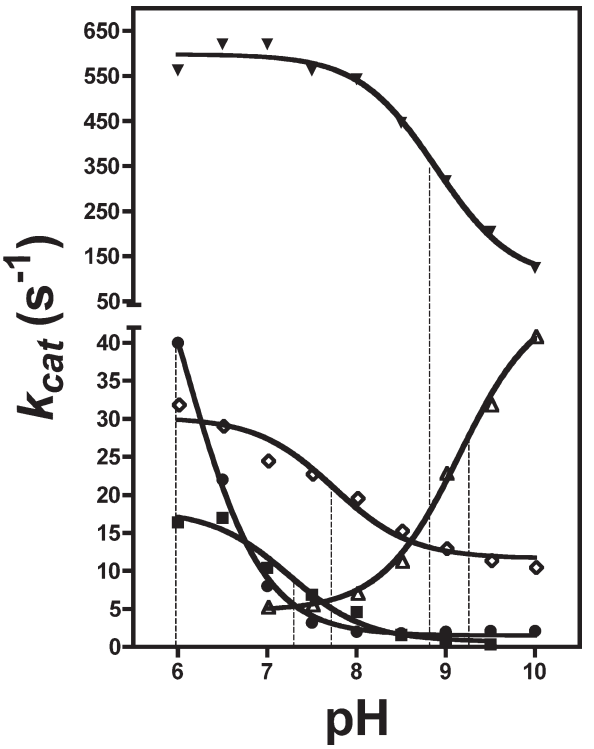

Figure 9. Effect of pH on the k_{cat} values of the native and the substituted enzymes with oNPG. Note that the vertical axis is segmented. Filled triangles, native β-galactosidase; filled squares, H418F-β-galactosidase; filled circles, H418N-β-galactosidase; open triangles, H418E-β-galactosidase at 150 m*M* NaCl; open diamonds, H418E-β-galactosidase at 2*M* NaCl.

Role of His-418 in catalysis

All three substitutions caused significant k_{cat} decreases (Table II). The following three findings show that this is due to decreases in k_3. (1) The k_{cat} values for oNPG and pNPG with each variant β-galactosidase were very similar (Table II). Since k_3 is the rate constant for the common degalactosylation step (Fig. 1), this suggests that k_3 is rate limiting. (2) Plots of $appk_{cat}$ vs. [1-propanol] or [Glc] gave linear increases in the rate. Results such as this show that the asymptote, $k_2k_4/(k_2 + k_4)$, of the hyperbola, described by Eq. (4), is very large and thus, that the values of k_2 and k_4 are much larger than k_{cat}.[23] Therefore, k_{cat} [Eq. (1)] is equal to k_3, and thus k_3 is very small. (3) The K_i values of three substrate analogs with hydrophobic aglycones (IPTG, PETG, t-oNPG) were large (Table III), suggesting that the *Ks* values for the nitrophenol (hydrophobic) substrates are also large. Therefore, the most plausible reason for the relatively small K_m values ($K_m = k_3K_s/(k_2 + k_3)$) of these substrates (Table II) is that the k_3 values are much smaller than k_2.

The pH profiles (see Fig. 9) suggest that the p*Ka* values of one or more groups on the enzyme were changed upon substituting for His-418. There are several titratable residues at the active site and this makes interpretation difficult—especially since the residues making up the pH profile are not yet definitively established. One group that must be important for the pH profiles is Glu-461 because it is a residue that is important for both binding and catalysis and whose chemistry is most likely to be influenced by His-418. The properties of Glu-416 (the third protein ligand of Mg^{2+}) could also be affected but it does not have any obvious substrate binding or catalytic role. Glu-461 is thought to undergo a p*Ka* shift between the free enzyme and the intermediate due to the changing charge state of Glu-537, explaining both the high and low pH dependence of native β-galactosidase.[30] In most of the pH profiles shown here, k_{cat} decreases with pH above pH 7 as with native enzyme, but the transition is lower by 1–3 pH units. The exception is H418E at low Na^+ for which k_{cat} increases with pH with a mid-point about 9.2; the reason for the increase is not obvious - possibly there is an ordering of the structure at higher pH, similar to that brought about by high Na^+. At high Na^+, the profile of this enzyme changes to be more similar to the other enzymes.

An important finding of this study is that the structure is essentially unchanged upon replacement with Glu or Asn but k_3 is much lower. Since His-418 does not directly interact with the substrate at any point during the reaction, the changes in the pH profile are most simply explained by His-418 optimizing the pKa of Glu-461 for binding and activity. The pKa optimization could occur indirectly via Mg^{2+} but His-418 and Glu-461 are also close enough (~2.9 Å) to each other for direct effects. Since the substitutions lower k_3, which is expected to depend on base catalysis, it supports the idea that the effect is due to altered base catalytic properties of Glu-461.

The H418 variants share some similarities with Mg^{2+} free native enzyme. The kinetic parameters are affected a similar amount (Table II). The pH profile of Mg^{2+} free enzyme[24] has the same shape as native but is shifted to lower pH by ~1 pH unit, not unlike H418E/2*M* NaCl and H418F, suggesting similar effects on the Glu-461 pKa. Because the pH profile of H418F is similar to the Mg^{2+} free enzyme, the effect of substituting Phe appears to be due to the loss of ability to bind Mg^{2+}. Furthermore, the instability of this enzyme is similar to Mg^{2+} free enzyme,[31,32] suggesting that the tendency for subunit dissociation of H418F is due, at least in part, to poor Mg^{2+} binding. However, there are also some differences between the H418 variants and Mg^{2+} free enzyme, as the latter is at least partially rate limited for galactosylation, and can therefore distinguish between ONPG and PNPG; unlike the H418 variants. Therefore, the H418 variants do not simply neutralize the role of the Mg^{2+}. It should also be mentioned that Phe can be modeled into position 418 without steric clashes with other protein atoms.

Another reason for the relatively low k_3 value may be the good binding of D-galactose. Galactose is

normally released readily. The relatively low K_i values for galactose with H418E- and H418N-β-galactosidase show that it is released more poorly. This could slow the degalactosylation reaction.

Role of His-418 in inducer formation

Allolactose formation by transgalactosylis with Glc as the acceptor is an important reaction because allolactose is the natural inducer of the lac operon.[33] If the affinity of Glc is high, the k_{cat} increase with Glc should be hyperbolic. However, addition of Glc (up to 1.25*M*) to the substituted enzymes (except H418E-β-galactosidase at 2*M* NaCl), caused the $appk_{cat}$ (oNPG) to increase in a first order fashion (data not shown). This and the calculation (see Results) of the Ki "values for H418E-ß-galactosidase in 2*M* NaCl (Ki″ >335 m*M*) shows that the K_i "values for Glc are very high; indicating that Glc binds very poorly to the acceptor site. This is consistent with the notion that the N_3 of His-418 in the native enzyme is involved in binding Glc as suggested by Juers *et al.*[3] on the basis of some weak electron density found when Glc was diffused into the active site of galactosylated native enzyme. The nitrogen (oxygen) of Asn-418 and the oxygen of Glu-418 are about 0.6 Å and 1.4 Å from the position occupied by N_3 of His, respectively, presumably affecting Glc binding at the acceptor site. In addition, an imidazole can more readily rotate[17] and accommodate Glc than can a Glu or an Asn. The better binding of Glc at high [Na^+] shows that part of the effect is order. It is significant that the Glc in the native enzyme can only be seen poorly in the acceptor site[3] while galactose can be easily visualized at this site in the H418E variant (see Fig. 5) despite overall poor resolution of this enzyme. The difference between Glc and galactose is in the orientation of the O_4 hydroxyl. This allows the interaction of galactose with Glu-418. Another role of His-418, therefore, is to bind Glc as an acceptor.

Materials and Methods

Mutagenesis

Site directed mutagenesis was accomplished by a modification of Kunkel's *dut*$^-$ *ung*$^-$ method[33,35] and/or using the Stratagene Quick-Change kit.[20]

Enzyme purification

The substituted β-galactosidases used for the kinetic analyses were purified as described previously[36] except that the enzymes were passed through Superose^{TM} 6 and Superose^{TM} 12 columns (joined in series) as an extra last step. Protein purity was determined by SDS-PAGE. The protein concentration was determined by the absorbance at 280 nm using an extinction coefficient of 2.09 cm^2/mg. SDS-PAGE (results not presented) showed that each substituted enzyme was >97% pure. The proteins used to prepare crystals were expressed and purified as previously reported.[20]

Crystallography

Crystals of H418N- and H418E-β-galactosidase were grown in space group $P2_12_12_1$ using the method and conditions previously reported.[20] Crystallization of H418F-β-galactosidase was unsuccessful. This variant was prone to dissociate during native gel electrophoresis although it was tetrametric when eluted from size exclusion columns. Diffraction data were collected on H418E- and H418N-β-galactosidase, as well as complexes between H418N-β-galactosidase and IPTG (125 m*M*) and between H418E-β-galactosidase and D-galactose (200 m*M*). The data were collected at ~100 K using 30% DMSO as the cyroprotectant.[20] Data were processed using Mosflm and Scala.[37–39] Refinement of the native, H418E- and H418N-ß-galactosidase was done with TNT[40] using native β-galactosidase (pdb code 1DPO) with active site waters and ions removed and His-418 truncated to Ala as a starting model. Initial rigid body refinement was followed with positional refinement. The mutated side chain was built in followed by positional and B-factor refinement (using the correlated B-factor restraint library in TNT). Any ligands were built in, followed by several rounds of solvent addition and removal with Arp,[41] alternating with positional and B-factor refinement. Rounds of model building alternating with more refinement resulted in the final model with the mutated side chains and modeled ligands. For H418E-ß-galactosidase in the presence of D-galactose, the crystals grew in space group $P2_1$ using the same conditions. Data were collected at ~100 K using 25% DMSO as the cryoprotectant and molecular replacement was done with Xtal View.[42] Xfit[42] and CNS[43] were used for rounds of refinement. Coordinates and structure factors have been deposited in the Protein Data Bank (accession codes 3DYP, 3DYO, 3DYM, and 3E1F).

Residues defining the walls of the active site and the opening to the active site pocket were determined using the program "Pocket."[44] Coordinate analyses were carried out using EdPDB.[45]

Enzyme assays

The assays were done in "TES Assay Buffer" (30 m*M* TES, 145 m*M* NaCl, pH 7.0 at 25°C) with oNPG and pNPG. The reaction rates were measured with a Shimadzu UV-2101 Spectrophotometer at 420 nm. The following extinction coefficients (pH 7.0) were used: oNP = 2.65 mM^{-1} cm^{-1}; pNP = 6.50 mM^{-1} cm^{-1}. Various amounts of Mg^{2+} or EDTA were added to the assays. EDTA was added when free Mg^{2+} concentrations below the endogenous levels were needed. The concentration of free Mg^{2+} was calculated from the endogenous Mg^{2+} levels, the concentration of EDTA added and the instability constants of EDTA•Mg^{2+} complexes at pH 7.0. Atomic Absorption Spectroscopy

(Perkin Elmer 5000) was performed to determine the endogenous Mg^{2+} concentrations. Unless otherwise stated, only effects at free Mg^{2+} concentrations of 10^{-5} M or less were measured so that only the effects of binding Mg^{2+} to the site ligated by residues at positions 416, 418, and 461 were considered. Control experiments did however show that substitutions for His-418 did not alter the effects of Mg^{2+} binding at the second Mg^{2+} site.[7]

Before analysis, the enzymes were eluted into TES Assay Buffer with a Sephadex G-25M column (Pharmacia). Enzyme was added in the absence of substrate and allowed to equilibrate in the TES Assay Buffer with the desired free Mg^{2+} concentration for 30 min before adding substrate (the substrate had the same Mg^{2+} concentrations) to begin the reaction (25°C).

Determination of kinetic constants

The K_m and k_{cat} values were obtained by non-linear regression of Michaelis-Menten data (using Prism™ 4 Software). Figure 1 illustrates the proposed mechanism of β-galactosidase in the presence of inhibitors. Almost all inhibitors of β-galactosidase are also acceptors that react in place of water. The thick arrows represent the reactions without inhibitor/acceptor (X). The following equations hold under those conditions:

$$k_{cat} = \frac{k_2 k_3}{k_2 + k_3} \quad (1)$$

$$K_m = \frac{k_3}{k_2 + k_3} K_s \quad (2)$$

The thin arrows in Figure 1 represent the additional reactions that take place in the presence of inhibitor/acceptor (X). The acceptors react to form galactosyl adducts (GA-X). Equation (3) accounts[2,46] for the acceptor effect (see Fig. 1) and was used to determine the values of the competitive inhibition constants (K_i).

$$\frac{appKm}{appk_{cat}} = \frac{K_m}{k_{cat}}\left(1 + \frac{[X]}{K_i}\right) \quad (3)$$

K_m and k_{cat} are the constants obtained in the absence of inhibitor/acceptor while appK_m and $appk_{cat}$ are the constants obtained in the presence of inhibitor/acceptor.

Equation (4) describes how $appk_{cat}$ changes as a function of the concentration of

$$appk_{cat} = \frac{\frac{k_2 k_3}{k_2 + k_3} + \frac{k_2 k_4}{k_2 + k_3}\frac{[X]}{K_i''}}{1 + \frac{k_2 + k_4}{k_2 + k_3}\frac{[X]}{K_i''}} \quad (4)$$

inhibitor/acceptor (X) in Figure 1[22,45] Estimates of $((k_2+k_3)K_i'')/(k_2+k_4)$ and of $k_2k_4/(k_2+k_4)$ can be obtained by plotting $appk_{cat}$ versus [X] and solving for these terms with Eq (4) by nonlinear regression. However, during this study, it was found that binding at the acceptor site was very poor and that most of the plots of $appk_{cat}$ versus [X] were, therefore, essentially linear. This suggests that the binding interaction is essentially first order (in other words, K_i" is very large).

Conclusions

There are a number of ways in which His-418 together with its liganded Mg^{2+} are important in the activity of ß-galactosidase.

1. When His-418 is replaced by Glu or Asn, the overall structure and the binding of Mg^{2+} are largely maintained, but the rate of degalactosylation becomes very slow and the pH profiles are different when Glu and Asn replace His-418 (probably due to effects on the pKa of Glu-461). This is strong evidence that a very important function of His-418 is to help maintain the correct chemical environment at the active site.
2. When His-418 is replaced by Phe, Mg^{2+} binding is essentially abolished and the enzyme behaves similar to the Mg^{2+}—depleted native enzyme.
3. The Glu-418 replacement and, to a lesser extent, the Asn-418 replacement result in disordering at the active site. This causes the nearby Na^+ to bind less well. High concentrations of Na^+ can partially compensate.
4. Substrate and substrate analog binding is poor when His-418 is replaced—most likely because of effects on Glu-461.
5. Binding of Glc as an acceptor is decreased significantly upon substitution for His-418 indicating that His-418 plays an important role in binding Glc as an acceptor.

References

1. Huber RE, Kurz G, Wallenfels K (1976) A quantitation of the factors which affect the hyrolase and trangalactosylase activities of ß-galactosidase (*E. coli*) on lactose. Biochemistry 15:1994–2001.
2. Huber RE, Gaunt MT (1983) Importance of hydroxyls at positions 3, 4, and 6 for binding to the galactose site of ß-galactosidase (*Escherichia coli*). Arch Biochem Biophys 220:263–271.
3. Juers DH, Heightman TD, Vasella A, McCarter JD, Mackenzie L,Withers SG Matthews BW (2001) A structural view of the action of Escherichia coli (lacZ) ß-galactosidase. Biochemistry 40:14781–14794.
4. Huber RE, Hakda S, Cheng C, Cupples CG, Edwards RA (2003) Trp-999 of ß-galactosidase (*Escherichia coli*) is a key residue for binding, catalysis, and synthesis of allolactose, the natural Lac operon inducer. Biochemistry 42: 1796–1803.
5. Tenu JP, Viratelle OM, Yon J (1972) Kinetic study of the activation process of ß-galactosidase from *Escherichia coli* by Mg2+. Eur J Biochem 26:112–118.
6. Huber RE, Parfett C, Woulfe-Flanagan H, Thompson DJ (1979) Interaction of divalent cations with ß-galactosidase (*Escherichia coli*). Biochemistry 18:4090–4095.
7. Sutendra G, Wong S, Fraser ME, Huber RE (2007) ß-Galactosidase (*Escherichia coli*) has a second catalytically

important Mg2+ site. Biochem Biophys Res Comm 352: 566–570.
8. Sinnott ML, Withers SG, Viratelle OM (1978) The necessity of magnesium cation for acid assistance of aglycone departure in catalysis by *Escherichia coli* (lacZ) ß-galactosidase. Biochem J 175:539–536.
9. Richard JP, Huber RE, Lin S, Heo C, Amyes TL (1996) Structure-reactivity relationships for ß-galactosidase (*Escherichia coli*. lac Z). III. Evidence that Glu-461 participates in Bronsted acid-base catalysis of ß-D-galactopyranosyl group transfer. Biochem 35:12377–12386.
10. Richard JP, McCall DA, Heo CK, Toteva MM (2005) Ground state, transition state, and metal-cation effects of the 2-hydroxyl group on ß-D-galactopyranosyl transfer catalyzed by ß-galactosidase (*Escherichia coli*, lacZ). Biochemistry 44:11872–11881.
11. Xu J, McRae MA, Harron S, Rob B, Huber RE (2004) A study of the relationship of interactions between Asp-201, Na+ or K+, and galactosyl C6-hydroxyl and their effects on binding and reactivity of ß-galactosidase. Biochem Cell Biol 82:275–284.
12. Edwards RA, Cupples CG, Huber RE (1990) Site directed mutants of ß-galactosidase show that Tyr-503 is unimportant in Mg2+ binding but that Glu-461 is very important and may be a ligand of Mg2+. Biochem Biophys Res Commun 171:33–37.
13. Jacobson RH, Zhang X-J, DuBose RF, Matthews BW (1994) Three-dimensional structure of ß-galactosidase from *E. coli*. Nature 369:761–766.
14. Roth NJ, Huber RE (1994) Site directed substitutions suggest that His-418 of ß-galactosidase (*E. coli*) is a ligand to Mg2+. Biochem Biophys Res Comm 201: 866–870.
15. Roth NJ, Huber RE (1996) Glu-416 of ß-galactosidase (*Escherichia coli*) is a Mg2+ ligand and ß-galactosidases with substitutions for Glu-416 are inactivated rather than activated by Mg2+. Biochem Biophys Res Commun 219: 111–115.
16. Potterton L, McNicholas S, Krissinel E, Gruber J, Cowtan K, Emsley P, Murshudov GN, Cohen S, Perrakis A, Noble M (2004) Developments in the CCP4 molecular-graphics project. Acta Crystallogr D 60: 2288–2294.
17. Glusker JP (1991) Structural aspects of metal binding to functional groups in proteins. Adv Prot Chem 42:1–76.
18. Gong L, Guo W, Xionga J, Lia R, Wu X, Li W (2006) Structures and stability of ionic liquid model with imidazole and hydrogen fluorides chains: density functional theory study. Chem Phys Lett 425:167–178.
19. Kraulis JP (1991) MOLSCRIPT: a program to produce both detailed and schematic plots of protein structures. J Appl Crystallogr 24:946–950.
20. Juers DH, Wigley RH, Zhang X, Huber RE, Tronrud DE, Matthews BW (2000) High resolution refinement of ß-galactosidase in a new crystal form reveals multiple metal binding sites and provides a structural basis for ⟨-complementation. Protein Sci 9:1685–1699.
21. Huber RE, Brockbank RL (1987) Strong inhibitory effect of furanoses and sugar lactones on ß-galactosidase of *Escherichia coli*. Biochemistry 26:1526–1531.
22. Petterson EF, Goddard TD, Huang CC, Couch GS, Greenblat DM, Meng EC, Ferrin TE (2004) UCSF Chimera—a visualization system for exploratory research and analysis. J Comput Chem 25:1605–1612.
23. Huber RE, Gaunt MT, Hurlburt KL (1984) Binding and reactivity at the "glucose" site of galactosyl-beta galactosidase (*Escherichia coli*). Arch Biochem Biophys 234:151.
24. Tenu JP, Viratelle OM, Garnier J, Yon J (1971) pH dependence of the activity of ß-galactosidase from *Escherichia coli*. Eur J Biochem 20:363–370.
25. Hill JA, Huber RE (1971) Effects of various concentrations of Na+ and Mg2+ on the activity of ß-galactosidase. Biochim Biophys Acta 250:530–537.
26. Hill JA, Huber RE (1974) The mechanism of Na+ activation of E.coli ß-galactosidase and the inhibitory effect of high concentrations of Mg^{2+} on this activation. Int J Biochem 5:773–779.
27. Case GS, Sinnott ML (1973) The role of magnesium ions in ß-galactosidase-catalysed hydrolyses. Biochem J 133: 99–104.
28. Viratelle OM, Yon JM (1973) Nucleophilic competition in some ß-galactosidase-catalyzed reactions. Eur J Biochem 33:110–116.
29. Huber RE, Gupta MN, Khare SK (1994) The active site and mechanism of the ß-galactosidase from *Escherichia coli*. Int J Biochem 26:309–318.
30. Richard JP (1998) The enhancement of enzyme rate accelerations by bronsted acid–base catalysis. Biochemistry 37:4305–4309.
31. Wickson VM, Huber RE (1970) The non-simultaineous dissociation and loss of activity of ß-galactosidase in urea. Biochim Biophys Acta 207:150–155.
32. Gallagher CN, Huber RE (1997) Monomer-dimer equilibrium of uncomplemented M15 ß-galactosidase from *Escherichia coli*. Biochemistry 36:1281–1286.
33. Jobe A, Bourgeois S (1972) Lac repressor-operator interaction VI. The natural inducer of the lac operon. J Mol Biol 69:397–408.
34. Kunkel TA (1987) Approaches to efficient site directed mutagenesis. Mol Biol Rep 1:1–2.
35. Kunkel TA, Roberts JD, Zakour RA (1987) Rapid and efficient site-specific mutagenesis without phenotypic selection. Methods Enzymol 154:367–382.
36. Cupples CG, Miller JH, Huber RE (1990) Determination of the roles of Glu-461 in ß-galactosidase (*E. coli*) using site-specific mutagenesis. J Biol Chem 265: 5512–5518.
37. Kabsch W (1988) Evaluation of single-crystal X-ray diffraction data from a position-sensitive detector. J Appl Cryst 21:916–924.
38. Leslie AGW, From chemistry to biology. In: Moras D, Podjarny AD, Thierry J-C, Eds. (1991), Crystallographic computing 5, Oxford: Oxford University Press, pp 50–61.
39. Evans PR (1993) In: proceedings of a CCP4 study weekendon data collection and processing, Daresbury: SERC Daresbury Laboratory, pp 114–122.
40. Tronrud DE (1997) TNT refinement package. Methods Enzymol 277:306–319.
41. Lamzin VS, Wilson KS (1993) Automated refinement of protein models. Acta Crystallogr D Biol Crystallogr 49: 129–147.
42. McRee D (1999) XtalView/Xfit–a versatile program for manipulating atomic coordinates and electron density. J Struct Biol 125:156–165.
43. Brünger AT, Adams PD, Clore GM, DeLano WL, Gros P, Grosse-Kunstleve RW, Jiang JS, Kuszewski J, Nilges M, Pannu NS, Read RJ, Rice LM, Simonson T, Warren GL (1998) Crystallography and NMR system: a new software suite for macromolecular structure determination. Acta Crystallogr D Biol Crystallogr 54:905–921.
44. Edelsbrunner H, Koehl P (2005) The geometry of biomolecular solvation. Discrete and Computational Geometry. (MSRI Publications) 52:243–275.
45. Zhang XJ, Matthews BW (1995) EDPDB: a multifunctional tool for protein structure analysis. J Appl Cryst 28: 624–630.
46. Deschavanne PJ, Viratelle OM, Yon JM (1978) Conformational adaptability of the active site of ß-galactosidase. J Biol Chem 253:833–837.